Multifunctional radio-frequency generator for cold atom experiments*

WEI Chun-hua (魏春华)[1,2] **and YAN Shu-hua** (颜树华)[1,2]**

1. Department of Instrument Science and Technology, College of Mechatronic Engineering and Automation, National University of Defense Technology, Changsha 410073, China

2. Interdisciplinary Center for Quantum Information, National University of Defense Technology, Changsha 410073, China

(Received 5 March 2016)

We present a low cost radio-frequency (RF) generator suitable for experiments with cold atoms. The RF source achieves a sub-hertz frequency with tunable resolution from 0 MHz to 400 MHz and a maximum output power of 33 dBm. Based on a direct digital synthesizer (DDS) chip, we implement a ramping capability for frequency, amplitude and phase. The system can also operate as an arbitrary waveform generator. By measuring the stability in a duration of 600 s, we find the presented device performs comparably as Agilent33522A in terms of short-term stability. Due to its excellent performance, the RF generator has been already applied to cold atom trapping experiments.

Document code: A **Article ID:** 1673-1905(2016)03-0173-5

DOI 10.1007/s11801-016-6050-1

In the experiments associated with cold atoms[1-3], for precisely controlling the frequency and amplitude of laser, fast switching and precise frequency tuning are usually achieved by acousto-optical modulator (AOM)[4,5], which is driven by radio-frequency (RF) signals. At present, many commercially available RF generators are difficult to control multiple AOMs in atomic physics experiments. For example, during the process of polarization gradient cooling (PGC) in a cold atom interferometry[6-8], for decreasing the temperature of the cold atoms, the detuning and the intensity of cooling laser must be changed simulataneously within a few milliseconds[9,10]. What's more, in order to optimize the process of velocity selection, some special shaped pulse waveforms[11,12] need to be produced to drive the AOM for controlling the amplitude of Raman lasers, while these waveforms are difficult to be achieved by using ordinary commercial signal source. The direct digital synthesizer (DDS) can be highly integrated on chip with excellent performance and is capable to provide a sine output with high frequency resolution, low phase noise, continuous phase and frequency modulated[13].

This paper presents a multifunctional RF generator based on the DDS technology, including the overall design of the RF source, detailed introduction of the system, and performance test. The needs of cold atom experiments can be satisfied very well, and the RF generator has been successfully used for trapping cold atoms in our laboratory.

The schematic configuration of the whole system is shown in Fig.1. It mainly includes three modules, which are power supply module, DDS core module, liquid crystal display (LCD) & key module. C8051F020 is selected as the microcontroller unit (MCU) of the system. LCD and keys are connected with MCU. When a key is pressed, MCU scans the key, and the key value is displayed on the LCD. MUC is communicated with the host computer via RS232. In order to generate the RF signal, we firstly need to set signal parameters through the keys, and then the control-parameters, such as frequency, phase and amplitude, required by the DDS (AD9910 from Analog Devices) are automatically generated by the MCU after calculation. MCU only needs to initialize DDS and sets corresponding register values of DDS. Then, DDS chip can output the desired waveform.

The AD9910 is a DDS with an integrated 14-bit digital-to-analog converter (DAC) supporting sample rates up to 1 GHz. The DDS/DAC combination forms a digitally programmable, high frequency and analog output synthesizer, which is capable of generating a frequency agile sinusoidal waveform at frequencies up to 400 MHz. The AD9910 is controlled by programming its internal control registers via a serial input/output (I/O) port. The three signal control parameters of frequency, phase and amplitude can be accessed to control the DDS. The DDS provides fast frequency hopping and frequency tuning

* This work has been supported by the National Natural Science Foundation of China (No.51275523), and the Specialized Research Fund for the Doctoral Program of Higher Education of China (No.20134307110009).

** E-mail: yanshuhua996@163.com

resolution with its 32-bit accumulator[14]. With the sample rate of 1 GHz, the frequency tuning resolution is 0.23 Hz.

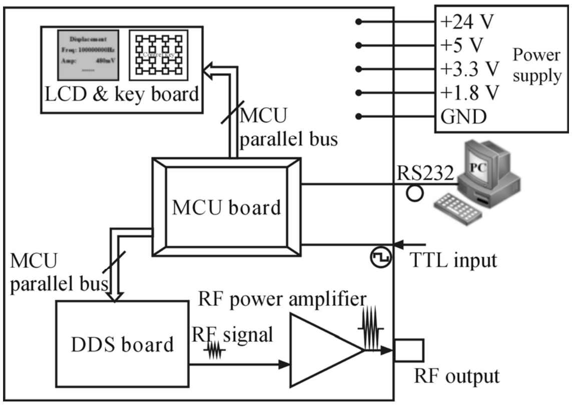

Fig.1 Schematic diagram of the system configuration

AD9910 supports multiple operating modes, and different modes can be enabled simultaneously, so an unprecedented flexibility can be provided for generating complex modulation schemes. We give full play to the performance of the DDS chip by coordinating the application of multiple modes. Through the combination of digital ramp modulation mode and output amplitude shift keying (OSK) function, we implement a ramping capability for frequency, phase and amplitude both independently and synchronously. AD9910 includes an integrated static random access memory (RAM) to support various combinations of frequency, phase and amplitude modulation. In RAM modulation mode, the DDS signal control parameters are stored in the internal RAM and played back upon command. Thus we can implement an arbitrary output waveform.

Because driving AOM requires a higher signal power beyond the capacity of DDS, a power amplifier with fixed gain is added after the output of DDS. AMPA-B-34 produced by AA Opto-Electronic is selected, whose gain is larger than 38 dB in the frequency range of 20—425 MHz. It can provide the necessary RF power to drive an AOM device.

To evaluate the overall performance of the proposed system, the RF generator is fully tested by the existing experimental conditions and commercial equipments. Finally, the proposed system is applied to the experiment of trapping cold atoms, which fully verifies the feasibility of our system.

A high resolution frequency counter (FCA3000 from Tektronix) is used here to measure the instantaneous frequency of the RF generator. The setting value of the frequency is changed by the keys, and the results about the output frequency of the system are shown in Tab.1. Because of the limited measurement range of FCA3000 (0—300 MHz), tests are carried out within 300 MHz. The maximum frequency error is 75.9 Hz, which occurs at the frequency of 300 MHz. There are two main reasons responsible for the frequency error, one is the frequency deviation of the reference source caused by frequency doubling of the reference source, and the other is the quantization error introduced by rounding parameter calculation program. We can easily get that the quantization error is less than 1 Hz. So the frequency deviation becomes the main source of frequency error. Accordingly, in order to improve the frequency accuracy, the crystal oscillator with high stability should be used as a reference source.

Tab.1 The frequency error of the proposed system

Setting value (MHz)	Measured value (MHz)	Error (Hz)
1	1.000 000 07	−0.07
10	9.999 999 52	0.48
50	49.999 997 8	2.20
100	99.999 993 61	6.39
150	149.999 974 3	25.70
200	199.999 969 7	30.30
250	249.999 948 1	51.90
300	299.999 924 1	75.90

Frequency stability is a key parameter to evaluate the system's quality. So we test the frequency stability of our system and then compare the results with a commercial signal source Agilent33522A. The output signal frequencies of our system and Agilent33522A are both set as 10 MHz. The frequency counter FCA3000 is used to measure the output frequency. We set the sampling interval as 1 s, and monitor continuously the frequency variation of Agilent33522A and our system for 10 min. Test results are shown in Fig.2, where the inset is a zoom-in result in the range of 425—475 s. We can get from Fig.2 that the maximum frequency variations of Agilent33522A and our system are 0.18 Hz and 0.26 Hz in 50 s, respectively. It's easy to find that the frequency stability of the proposed system approaches that of the commercial signal source Agilent33522A.

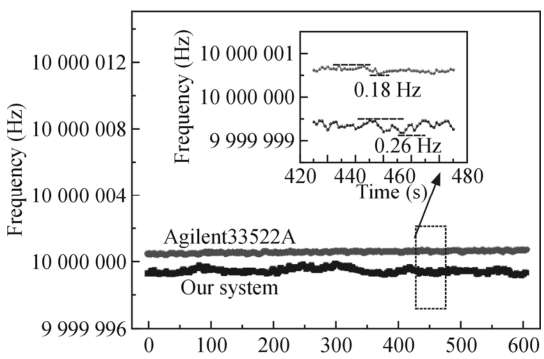

Fig.2 Test results of frequency stability of Agilent33522A and the proposed system

The output power as a function of the DDS frequency is shown in Fig.3. The output power of the signal can be controlled by adjusting the amplitude of the output signal through the keys. Fig.3(a) shows the original output power of AD9910 directly. Because driving AOM requires higher signal power, a power amplifier with fixed gain (AMPA-B-34) is added after the output of DDS. Fig.3(b) shows the output power after AMPA-B-34, and the roll-off at low and high frequency is due to the finite bandwidth of AMPA-B-34.

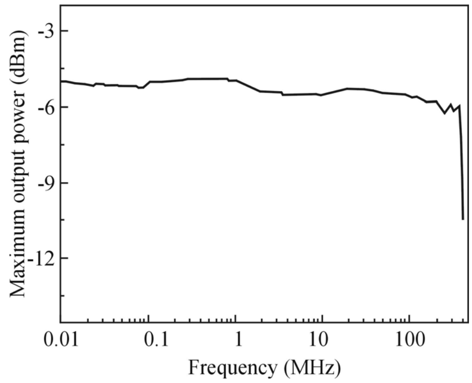

(a) Original output power of AD9910

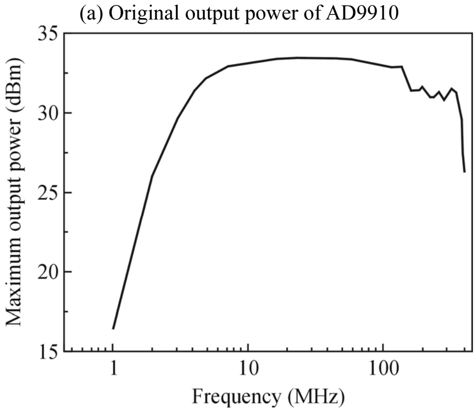

(b) Output power after amplifier AMPA-B-34

Fig.3 Maximum output power as a function of the DDS frequency

In some scenarios, we need to change the detuning and intensity of the laser in our experiment. For example, in the process of polarization gradient cooling (PGC), it requires that the frequency and amplitude of the driving signal ramp simultaneously. In this case, synchronous ramping of frequency and amplitude is expected.

According to the prompt on the LCD, the ramp parameters, such as start frequency, end frequency and ramp time, are set by keys. The trigger of starting ramp is provided by an external transistor-transistor logic (TTL) signal.

We connect FCA3000 with a host computer through a USB cable, and record the process of frequency ramping. The frequency ramping results are shown in Fig.4. In Fig.4(a), the start frequency is 50 MHz, the end frequency is 150 MHz, and ramp time is 2 ms. In Fig.4(b), the starting frequency is 270 MHz, the end frequency is 30 MHz, and the ramp time is 2 ms. The experimental results from Fig.4 show that the output frequency of our system can be swept smoothly.

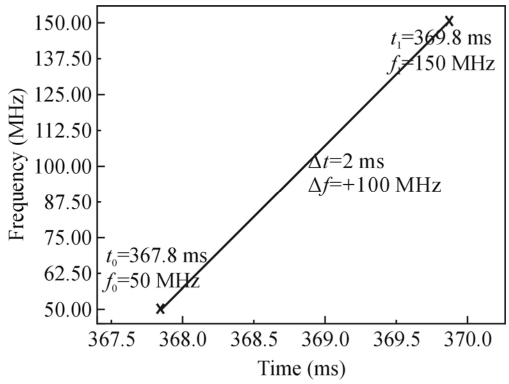

(a) Forward frequency ramping

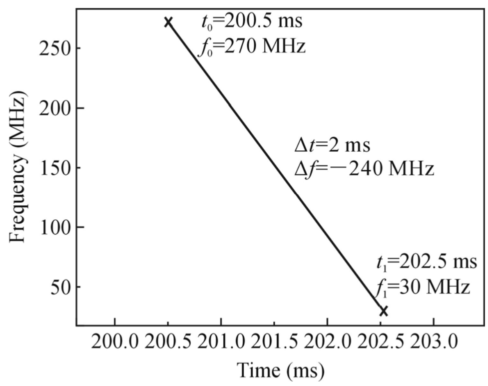

(b) Backward frequency ramping

Fig.4 Experimental result of frequency ramping

The process of amplitude ramping is recorded by a digital phosphor oscilloscope (Tektronix, DPO2024). We set the ramp time as 20 ms, the start amplitude as 560 mV (PV value) and the end amplitude as 0. The test results are shown in Fig.5. It can be found from Fig.5 that the output amplitude of our system can also be changed smoothly.

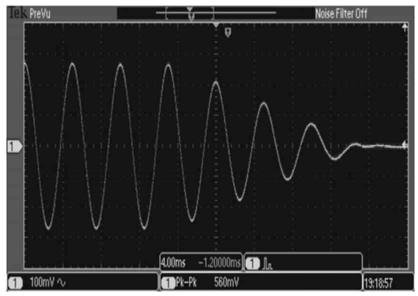

Fig.5 Experimental result of amplitude ramping

Fig.6 shows a ramping capability for both frequency and amplitude simultaneously. We note that the DDS chip is capable of ramping both the amplitude and frequency simultaneously through the combination of digital ramp modulation mode and OSK function. The test results show that simultaneous frequency and amplitude ramping can be implemented at the same time.

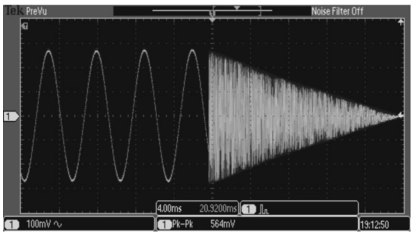

Fig.6 Experimental result of simultaneous amplitude and frequency ramping

The same as amplitude and frequency ramping, the phase ramping parameters are also set by keys, and the trigger signal of starting ramp is provided by an external TTL signal. Fig.7 shows a capability of phase ramping (Trace 1) compared with a fixed reference (Trace 2). We set the ramp phase as 180° in Fig.7(a) and 360° in Fig.7(b). The experimental results show that the phase ramping capability is implemented successfully in this work.

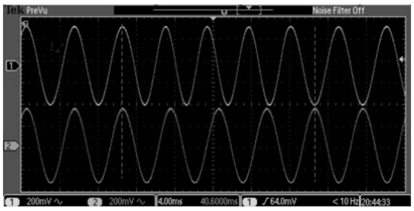

(a)

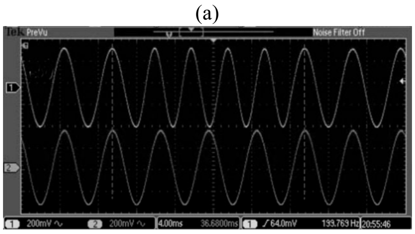

(b)

Fig.7 Experimental results of phase ramping with ramp phase of (a) 180° and (b) 360°

The AD9910 includes a 1 024×32-bit RAM. The RAM mode of AD9910 is widely applied in frequency and amplitude sweeping, arbitrary waveform generation and so on.

In Raman type atom interferometer, a defined pulse shape of $f(t)$ can be implemented by adjusting the intensity of the two counter-propagating Raman beams (using AOMs) to trace the absolute value $|f(t)|$, while keeping the intensity ratio constant to cancel the influence of alternating current (AC) Stark effect. And for negative values in $f(t)$, it represents an amplitude of $|f(t)|$ with a phase jump of π, and can be achieved by the optical phase lock loop. By using our RF generator, an implementation of Reburp pulse[15] is shown in Fig.8.

After the overall test of our system, we use the RF generator to drive the AOM in the experiment of trapping cold atoms. For atom trapping, we need lasers nearly resonant to two transitions from the hyperfine ground states as shown in Fig.9. We use two lasers locked to these transitions. A Toptica TA Pro laser is used for trap and probe laser, and a Toptica DL 100 laser is used for the repump laser.

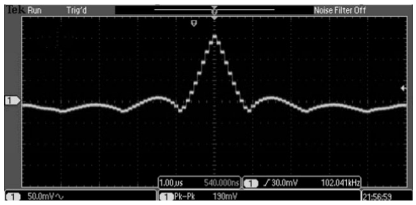

(a)

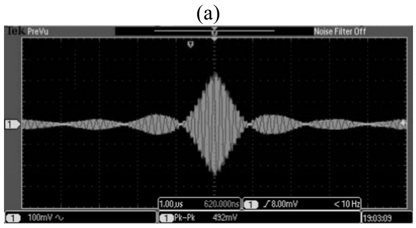

(b)

Fig.8 Reburp pulse implementation: the absolute value of (a) defined Reburp pulse and (b) Reburp pulse with a 100 MHz frequency modulation

The TA pro laser is locked to the $5S_{1/2}$, F=2→|$5P_{3/2}$, F=2,3 cross-over peak after passing through a double pass AOM (MT200, AA) driven by 200 MHz RF signal. The locked laser is split into two beams with different intensity components. A second double pass AOM (MT110, AA) is used to trap the atoms, which operates at 100 MHz to form a 12 MHz detuning below the F=2→F'=3 transition. The probe light is 2 MHz below the atomic transition after passing through a double pass AOM (MT110, AA) driven at 95 MHz. The DL 100 laser is locked to the $5S_{1/2}$, F=1→|$5P_{3/2}$, F=1,2 cross-over peak. After passing through a single pass AOM (MT80, AA) driven at 78.5 MHz, we get the repump light. The repump laser make the F=1 ground state empty, the trap laser cycles atoms on the trapping transition, and the probe is used to observe the absorption spectrum.

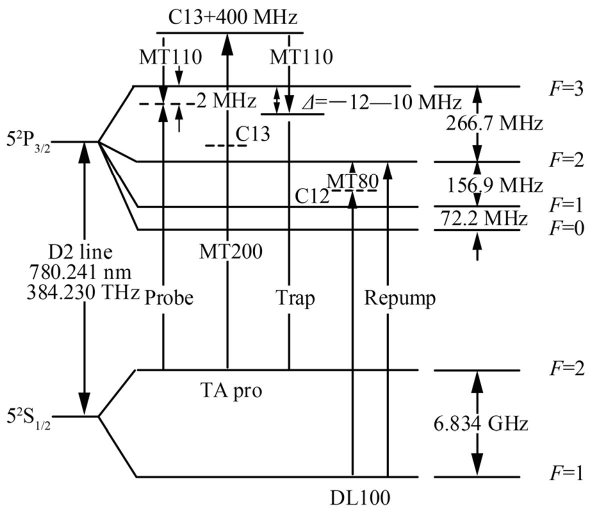

Fig.9 Atomic energy level structure of 87Rb and the laser frequencies of trapped cold atoms

Fig.10 shows a trapped atom cloud detected by charge-coupled device (CCD). After preliminary calculations, we get that the atom number of the trapped atom cloud is about 5×10^7, which further verify the feasibility of our RF generator.

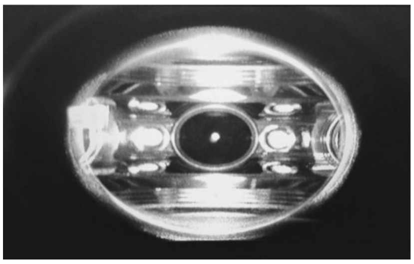

Fig.10 Trapped atom cloud detected by CCD

In conclusion, we present a multifunctional RF generator, which achieves a sub-hertz frequency with tunable resolution from 0 MHz to 400 MHz and a maximum output power of 33 dBm. We implement a ramping capability for frequency, amplitude and phase independently as well as a ramping capability for both frequency and amplitude synchronously. The output of arbitrary waveforms makes the system suitable for experiments with cold atom. All the experimental results prove the competent performance of our system, which is promising as a low-budget choice in the fields of AOM driving, cold atom trapping, cold atom interferometry, and so on.

References

[1] Peters A., Chung K. Y. and Chu S., Nature **400**, 849 (1999).

[2] Müller T., Gilowski M., Zaiser M., Berg P., Schubert Ch., Wendrich T., Ertmer W. and Rasel E. M., The European Physical Journal D **53**, 273 (2009).

[3] Zhou L., Xiong Z. Y., Yang W., Tang B., Peng W. C., Wang Y. B., Xu P., Wang J. and Zhan M. S., Chinese Physics Letters **28**, 013701 (2011).

[4] Cao Q., Luo X. Y., Gao K. Y., Wang X. R., Chen D. M. and Wang R. Q., Chinese Physics B **21**, 043203 (2012).

[5] Anderson M. H., Petrich W., Ensher J. R. and Cornell E. A., Physical Review A **50**, R3597 (1994).

[6] Butts D. L., Kotru K., Kinast J. M., Radojevic A. M., Timmons B. P. and Stoner R. E., Journal of the Optical Society America B **30**, 922 (2013).

[7] Zhou M. K., Duan X. C., Chen L. L., Luo Q., Xu Y. Y. and Hu Z. K., Chinese Physics B **24**, 050401 (2015).

[8] Cao Ye, Liu Ce and Tong Zheng-rong, Optoelectronics Letters **10**, 401 (2014).

[9] P. J. Ungar, D. S. Weiss, E. Riis and S. Chu, Journal of the Optical Society America B **6**, 2058 (1989).

[10] K. B. Davis, M. -O. Mewes, M. R. Andrews, N. J. van Druten, D. S. Durfee, D. M. Kurn and W. Ketterle, Phys. Rev. Lett. **75**, 3969 (1995).

[11] Kovachy T., Chiow S. and Kasevich M. A., Physical Review A **86,** 011606 (2012).

[12] Goswami D., Physics Reports **374**, 385 (2003).

[13] Yuan Jin, Ning Ti-gang, Li Jing, Li Yue-qin, Chen Hong-yao and Zhang Chan, Optoelectronics Letters **11**, 207 (2015).

[14] http://www.analog.com/media/en/technical-documentation/data-sheets/AD9910.pdf

[15] Geen H. and Freeman R., Journal of Magnetic Resonance **93**, 93 (1991).